Proceedings Paper:
Onyeji, L and Kale, G orcid.org/0000-0002-3021-5905 (2017) Corrosion performance of high strength-low alloy steels in aerated and CO_2 saturated Lyman and Fleming solutions. In: Proceedings of the Materials Science and Technology Conference and Exhibition 2017. MS&T17: Materials Science and Technology Conference and Exhibition 2017, 08-12 Oct 2017, Pittsburgh, PA, USA. MS&T17 , pp. 1103-1108. ISBN 978-1-5108-5058-3

https://doi.org/10.7449/2017/MST_2017_1103_1108

CORROSION PERFORMANCE OF HIGH STRENGTH-LOW ALLOY STEELS IN AERATED AND CO_2 SATURATED LYMAN AND FLEMING SOLUTIONS.

Lawrence Onyeji and Girish Kale

Institutes for Materials Research, School of Chemical and Process Engineering, University of Leeds, Leeds, LS2 9JT, United Kingdom

Key Words: Aerated Solution; Calcareous Deposits; CO_2 saturated solutions; Corrosion Rate; Dissolved Oxygen; High Strength-Low Alloyed Steels; Lyman and Fleming solutions;.

ABSTRACT

Aerated and CO_2 saturated Lyman and Fleming solutions were used as electrolytes to investigate the corrosion susceptibility of three high strength low alloy steels (HSLA) designated as Steel A, Steel B and Steel C. API 5L X65 carbon steel was used as reference specimen. Electrochemical Polarization (LPR and Tafel Extrapolation) and surface analysis (SEM/EDAX and XRD) techniques were used for this investigation. The results of linear polarization resistance (LPR) and potentiodynamic polarization corroborated each other presenting the corrosion performance (CP) of the steels in a descending order of $CP_{Steel\ C} > CP_{Steel\ B} > CP_{X65} > CP_{Steel\ A.}$ The results also revealed a more severe corrosion attack averaging about 35% for all the steels in the aerated than in the CO_2 saturated Lyman/Fleming solutions. This was attributed to the absence of dissolve oxygen (DO) and the covering of the surface of the specimens by CO_2 gas in CO_2 saturated solution. On the other hand, the presence of DO which is a precursor for cathodic reduction and for the formation of calcareous deposits, initiated an early rapid corrosion attack culminating to higher corrosion rates within the 24 hours of this work. The chemical composition and microstructures of the steels contributed significantly to the witnessed corrosion behaviour. The API XL X65 carbon steel showed almost a comparable corrosion resistance with Steel A but differ significantly with Steel B and Steel C in both aerated and CO_2 saturated Lyman and Fleming solutions.

1.0 INTRODUCTION:

High strength-low alloy steel, because of its excellent combination of mechanical properties such as strength, toughness, formability and weldability [1], have found increasing applications as piping and process equipment for extraction, production and transportation in oil and gas industry [1-4]. However, literatures [5-12] have reported that oilfield environments consist of divers corrosion species such as carbon dioxide (CO_2), hydrogen sulphide (H_2S), elemental sulphur, water, organic acids, bacteria, inorganic chloride salts (sodium chloride, calcium chloride, magnesium chloride), dissolved oxygen, biological activity and pollutants. Thus these facilities are subjected to various type of corrosion attacks such as sweet (CO_2) corrosion, sour (H_2S) corrosion, seawater corrosion and/or atmospheric corrosion thereby challenging the integrity and reliability of the materials. These attacks if not mitigated may lead to equipment failure with its attendant consequences [11].

Seawater is a complex chemical system which is very difficult to exactly duplicate and sustain in laboratories due to the variabilities of the dissolved substances and the activities of living organisms [5, 13, 14]. This has led to the development of different formulae and compositions for simulating seawater by many researchers [13]. Lyman and Fleming formula is one of the most widely used recipes for simulated seawater [13]. Also 3.5 wt% NaCl solution is frequently used to simulate seawater for laboratory purposes [5, 13-16]. However, many authors [5, 14, 17, 18] have reported that seawater has lower corrosion rate on carbon steel than 3.5 wt% NaCl solution which is ascribed

to the presence of certain cations such as Ca^{2+} and Mg^{2+}. These cations form $CaCO_3$ and $Mg(OH)_2$ precipitates which promote physical barrier against oxygen diffusion from the bulk solution to the surface of the steels thereby reducing corrosion rate [5, 14, 17, 18].

In this work, four high strength-low alloyed steels, three of which are branded steels, were subjected to electrochemical corrosion tests in aerated and CO2 saturated Lyman and Fleming solution so as to investigate the corrosion performance of the steels and to validate the corrosivity of the two corrosion environments.

2.0 Materials and Experiments

Lyman and Fleming solutions were used to prepare simulated seawater. Two environmental conditions namely aerated and CO_2 saturated solutions were deployed. The four high strength-low alloy steels were metallographically prepared and corroded using the conventional three electrode cell with platinum as counter electrode, Ag/AgCl (sat. KCl) electrode as reference electrode while the steel specimens were the working electrodes. Linear polarization resistance (LPR) was conducted after 13 minutes OCP at a scan rate 0.25 mV/cm^2 and a scan range of $\pm$15mV versus OCP and for 24 hours. This was followed by Potentiodynamic polarization at a sweep range of $\pm$250 mV versus OCP and a sweep rate of 0.5 mV/cm^2.

3.0 Results and Discussion

3.1 Linear Polarization Resistance (LPR)

Figure 1 shows the LPR corrosion rate of the steels corroded in unbuffered aerated and CO2 saturated simulated seawater at 25^{0}C and for 24 hours.

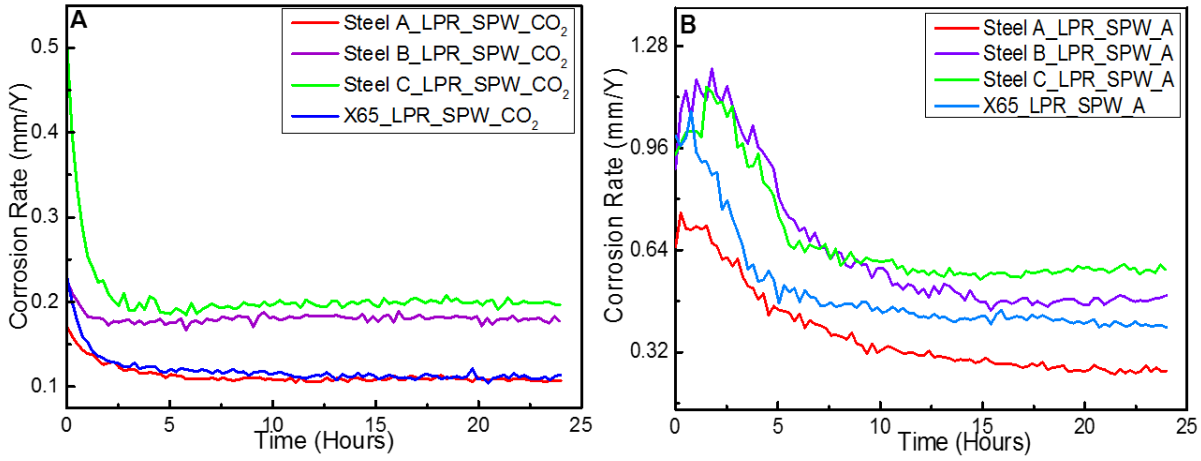

Figure 1: LPR Corrosion Rate of the Steels in (A) CO_2 Saturated and (B) Aerated Sea Water at 25C and for 24

It can be deduced from Figure 1A that all the steel specimens on immersion in the CO_2 saturated Lyman and Fleming solution began to corrode at a relatively high corrosion rate but decreased rapidly to a seemingly steady rate within the first 3 to 4 hours depending on the specimen. This rapid decrease in corrosion rate according to Davis [16] and Tait [19] can be ascribed to the dissolution of the air-formed oxide film on the surface of the specimens which hinders metal dissolution. Figure 1B on the other hand shows the LPR corrosion rate of the steels immersed in aerated Lyman and Fleming solutions. A closer look at Figure 1B revealed that there was an initial increase in corrosion rate which formed a threshold within the period of 0.5 to 2.5 hours of immersion depending on the specimen. This initial increase in corrosion rate signified that the air-formed oxide film on the surface of the specimens were porous and so could not protect the steels from further corrosion [16, 19]. This was followed by a rapid decrease in corrosion rate and then relatively and almost appearing stable throughout the remaining duration for the test. All the specimens displayed the same corrosion trend with Steel A appearing stable at 0.3 mm/y, Steel B at 0.5 mm/y, Steel C at 0.64 mm/y and X65 at

0.48 mm/y. In general, Figure 1 vividly showed that the corrosion rate for all the specimens in both aerated and CO_2 saturated Lyman and Fleming solutions can be ranked in ascending order as $CR_{Steel\ A} < CR_{X65} < CR_{Steel\ B} < CR_{Steel\ C}$.

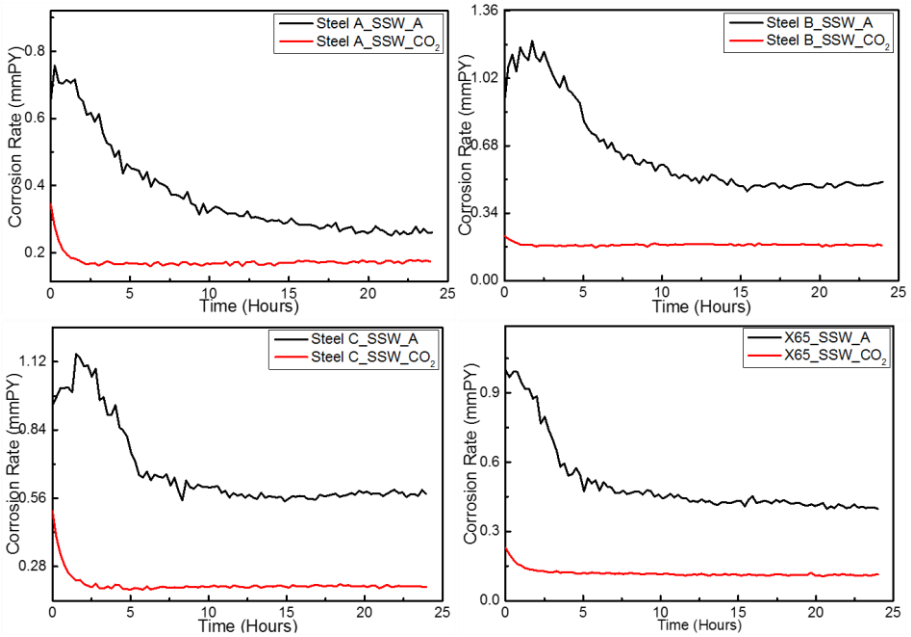

Figure 2: Comparison of LPR Plots of the Samples in Aerated and CO_2 Saturated Seawater

Figure 2 compares the LPR corrosion rate of individual specimen in aerated and CO_2 saturated Lyman and Fleming solutions. This figure revealed that the corrosion rate for all the specimens is higher in aerated Lyman and Fleming solution than in CO_2 saturated Lyman and Fleming solution. This difference in corrosion rate ranged from about 50% for Steel A to about 70% for Steel B. This high corrosion rate in aerated solutions can be ascribed to the presence of dissolved oxygen (DO) which is a precursor for cathodic reduction and the formation of calcareous deposits. The dissolved oxygen (DO) initiated an early rapid corrosion attack culminating to higher corrosion rate prior to the development of corrosion products [17, 18]which according to Elbeik, et al [17] can completely cover the surface of the metal with corrosion products ($CaCO_3$) within 66 days of immersion.

3.1.2 Potentiodynamic Polarization (Tafel Plots)

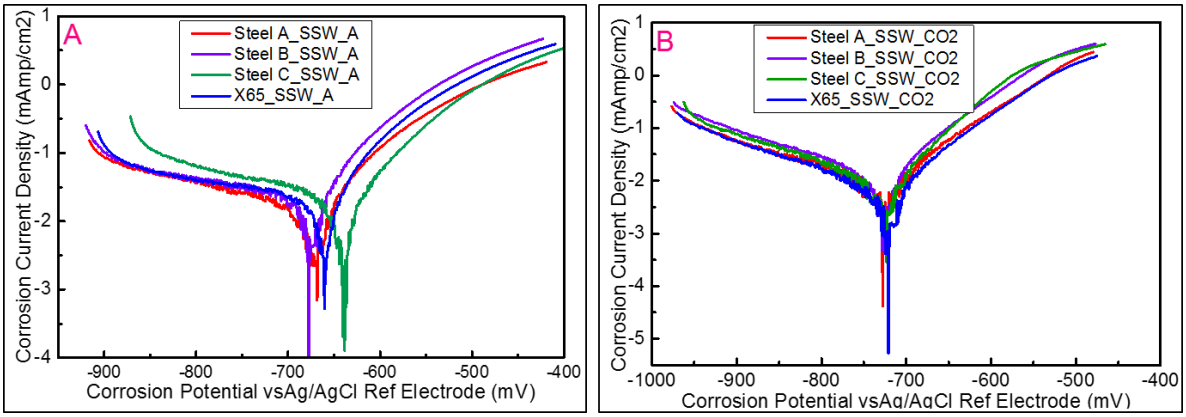

Figure 3: Tafel Plots of Specimens in (A) Aerated and (B) CO_2 Saturated Simulated Seawater

Figure 3 shows Tafel plots for all the specimens in both aerated and CO_2 saturated Lyman and Fleming solutions. From this figure, it can be observed that all the specimens exhibited the same corrosion behaviour of a continuous increase in anodic current with increase in corrosion potentials

thus displaying a well-defined Tafel region in both solutions. This suggests that passive film was not formed [20-22]. On the other hand, the cathodic polarization curves for all the steels showed a mixed activation- and diffusion- controlled characteristics for all the steels. However this is more pronounced in the aerated environment wherein limiting diffusion current density was observed. Henriquez, et al [23] ascribed this behaviour to the mass-transport limitation (seemingly current plateau) of the reduction reaction. The variations in corrosion behaviour in the two media are made more vivid in Figure 4 which compared the Tafel plots and in Table 1 which shows the values of Tafel extrapolation parameters in unbuffered aerated seawater solutions at 25^0C.

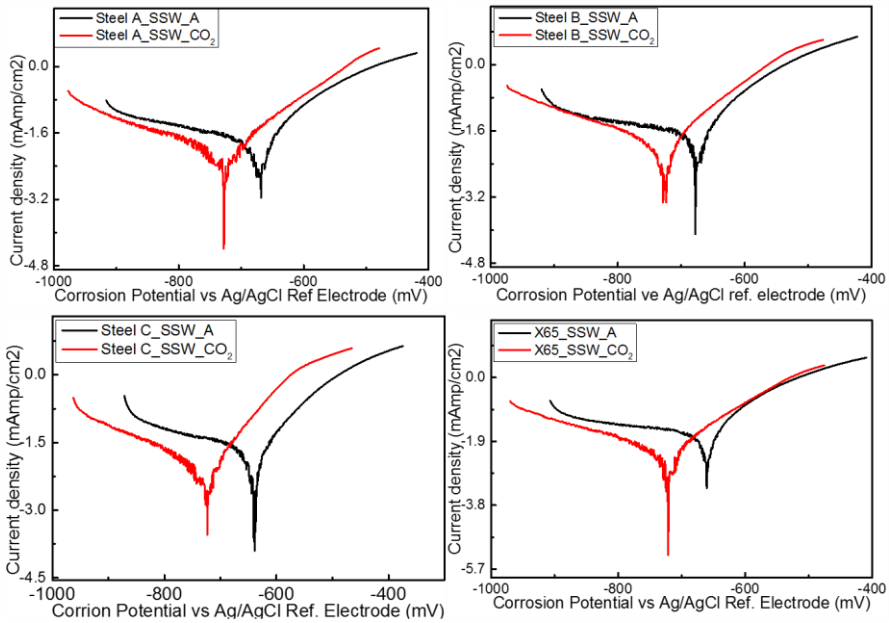

Figure 4: Comparison of Tafel Plots of the Steels in Aerated and CO_2 Saturated Seawater

A closer look at Figure 4 revealed that the corrosion potentials shifted towards the negative direction in CO_2 saturated solutions (ie has more negative potential) than the aerated solution. The cathodic polarization curves of the steel in aerated solutions also displayed more limiting diffusion current density which can be attributed to the presence of dissolved oxygen (DO) than in the CO_2 saturated solutions. These must have facilitated the higher corrosion rate witnessed in aerated solutions than in the CO_2 saturated solutions. The values of cathodic Tafel constants (β_c) as shown in Table 1 for all the specimens are more than the corresponding anodic constants. This behaviour according to Yin, et al [24] is an indication that the overall corrosion processes were controlled by cathodic reactions. This is elucidated by higher cathodic current curves in the aerated solutions than in CO_2 saturated solutions as depicted in Figure 4.

Table 1: Tafel Extrapolation Parameters of Steels in Aerated Simulated Sea Water

Samples	Ecorr (mV)	Icorr (µAmp/cm2)	βa (mV/decade)	βc (mV/decade)	Rp (Ω)	CR (mm/Y)
Steel A	-668	9.5	57	165	1936.37	0.110
Steel B	-676	10.4	48	102	1362.77	0.121
Steel C	-639	15.5	72	181	1443.00	0.180
X65	-661	9.7	45	100	1389.25	0.113

The SEM micrographs of the specimens corroded in CO_2 saturated Lyman Fleming solution showed corrosion product free surface. This was supported by the XRD analysis which displayed only Fe peak. On the other hand, the SEM micrographs of the specimens corroded in aerated Lyman and

Fleming solutions revealed surfaces with non-uniform deposition of corrosion products which are believed to be $CaCO_3$ [17, 18]. Many authors [5, 14, 17, 18] have reported that this $CaCO_3$ (part of calcareous deposit) forms physical barrier to the diffusion of dissolved oxygen from the bulk solution to the steel surface thus preventing and/or reducing corrosion rate. This behaviour occurs at about 66 days of immersion during which $CaCO_3$ deposit is uniform, dense and cover the surface of the steels.

CONCLUSION

Lyman and Fleming solution which is a widely accepted recipe for simulated seawater solution was used to investigate the corrosion susceptibility of three micro-alloyed steels and the fourth one as reference electrode. The tests were conducted in aerated and CO_2 saturated Lyman and Fleming solutions using linear polarization resistance, potentiodynamic polarization, and weight loss techniques. From the results of these tests, the following conclusions can be drawn.

- The corrosion attack for all the steels in the aerated solution was about 35% more than that in the CO_2 saturated solutions. This was attributed to the presence of dissolve oxygen (DO) which is a precursor for cathodic reduction and which enhances metal dissolution due to the corresponding anodic reactions. In the CO_2 environments, the surface of the steels were covered by adsorbed CO_2 gas thus reducing the surface area in contact with corrosion species and so decreases corrosion attack.
- Although DO also enhances the formation of calcareous deposits, these deposits were porous, non-adhesive and therefore could not form adequate physical barrier against corrosion attack.
- The results of all the corrosion techniques used corroborated each other presenting the corrosion rate (CR) of the steels in a descending order of $CR_{Steel\ C} > CR_{Steel\ B} > CR_{X65} > CR_{Steel\ A}$. This variation in corrosion rate can be attributed to the chemical composition and microstructures of the steels.
- The API XL X65 carbon steel showed almost a comparable corrosion rate with Steel A but about 7% and 60% better than Steel B and Steel C in aerated and CO_2 saturated Lyman and Fleming solutions respectively.

ACKNOWLEDGEMENT

- We wish to acknowledge and appreciate the sponsorship of this work by the Petroleum Technology Development Fund (PTDF), Abuja, Nigeria.
- For supplying the micro alloyed steels used in this work, we say thank you to Professor B. kermani.

REFERENCE

1. Davis, J.R., Alloying: understanding the basics. 2001: ASM international.
2. Edmonds, D.V. and R.C. Cochrane, The effect of alloying on the resistance of carbon steel for oilfield applications to CO2 corrosion. Materials Research, 2005. **8**(4): p. 377-385.
3. Hernandez, J., A. Muñoz, and J. Genesca, Formation of iron-carbonate scale-layer and corrosion mechanism of API X70 pipeline steel in carbon dioxide-saturated 3% sodium chloride. Afinidad, 2012. **69**(560).
4. Mora-Mendoza, J. and S. Turgoose, Fe 3 C influence on the corrosion rate of mild steel in aqueous CO 2 systems under turbulent flow conditions. Corrosion Science, 2002. **44**(6): p. 1223-1246.
5. Moller, H., E. Boshoff, and H. Froneman, The corrosion behaviour of a low carbon steel in natural and synthetic seawaters. Journal-South African Institute of Mining and Metallurgy, 2006. **106**(8): p. 585.

6. Castaño, J., Botero, CA., Restrepo, AH, Agudelo, EA, ., Correa, E.,Echeverría, F., Atmospheric corrosion of carbon steel in Colombia. Corrosion Science, 2010. **52**(1): p. 216-223.
7. Chen, Y., Tzeng, HJ., Wei, LI., Wang, LH., Oung, JC., Shih, HC, Corrosion resistance and mechanical properties of low-alloy steels under atmospheric conditions. Corrosion Science, 2005. **47**(4): p. 1001-1021.
8. Mameng, S.H., A. Bergquist, and E. Johansson. Corrosion of Stainless Steel in Sodium Chloride Brine Solutions. in CORROSION 2014. 2014. NACE International.
9. Ilman, M., Analysis of internal corrosion in subsea oil pipeline. Case Studies in Engineering Failure Analysis, 2014. **2**(1): p. 1-8.
10. Nabhani, F., A. Jasim, and S. Graham. Electrochemical Behaviour of Low Carbon Steel in Aqueous Solutions. in Proceedings of the World Congress on Engineering. 2007.
11. Liu, Y., Zhang, Bo., Zhang, Yinlong., Ma, Lili., Yang, Ping., Electrochemical polarization study on crude oil pipeline corrosion by the produced water with high salinity. Engineering Failure Analysis, 2016. **60**: p. 307-315.
12. Tawancy, H., L.M. Al-Hadhrami, and F. Al-Yousef, Analysis of corroded elbow section of carbon steel piping system of an oil–gas separator vessel. Case Studies in Engineering Failure Analysis, 2013. **1**(1): p. 6-14.
13. Sverdrup, H.U., M.W. Johnson, and R.H. Fleming, The Oceans: Their physics, chemistry, and general biology. Vol. 7. 1942: Prentice-Hall New York.
14. Möller, H., The influence of Mg 2+ on the formation of calcareous deposits on a freely corroding low carbon steel in seawater. Corrosion science, 2007. **49**(4): p. 1992-2001.
15. Denny, A.J., Principles and prevention of corrosion. Prentice-Hall Inc., Upper Saddle River, NJ, 1996: p. 76-90.
16. Davis, J.R., Corrosion: understanding the basics. 2000: ASM International.
17. Elbeik, S., A. Tseung, and A. Mackay, The formation of calcareous deposits during the corrosion of mild steel in sea water. Corrosion science, 1986. **26**(9): p. 669-680.
18. Hartt, W.H., C.H. Culberson, and S.W. Smith, Calcareous deposits on metal surfaces in seawater—a critical review. Corrosion, 1984. **40**(11): p. 609-618.
19. Tait, W.S., An introduction to electrochemical corrosion testing for practicing engineers and scientists. 1994: Clair, Racine, Wis.
20. Yu, C., X. Gao, and P. Wang, Electrochemical Corrosion Performance of Low Alloy Steel in Acid Sodium Chloride Solution. Electrochemistry, 2015. **83**(6): p. 406-412.
21. Sherif, E.-S.M., A comparative study on the electrochemical corrosion behavior of iron and X-65 steel in 4.0 wt% sodium chloride solution after different exposure intervals. Molecules, 2014. **19**(7): p. 9962-9974.
22. Choi, Y.-S., J.-J. Shim, and J.-G. Kim, Corrosion behavior of low alloy steels containing Cr, Co and W in synthetic potable water. Materials Science and Engineering: A, 2004. **385**(1): p. 148-156.
23. Henriquez, M., et al., Electrochemical investigation of the corrosion behavior of API 5L-X65 carbon steel in carbon dioxide medium. Corrosion, 2013. **69**(12): p. 1171-1179.
24. Yin, Z., Wang, XZ., Gao, RM., Zhang, SJ., Bai, ZQ., Electrochemical behavior and mechanism of CO2 corrosion on P110 steel in simulated oilfield solution. Anti-Corrosion Methods and Materials, 2011. **58**(5): p. 227-233.